NATURAL MICRON-SCALE ROUGHNESS OF CHEMICAL SEDIMENTARY ROCKS AND EFFECTS ON THERMAL INFRARED SPECTRA. C. Hardgrove[1] and A. D. Rogers[2], [1]Arizona State University, School of Earth and Space Exploration, Arizona State University, ISTB4 Bldg 75, 781 E Terrace Rd, Tempe, Arizona, 85287-6004 (craig.hardgrove@asu.edu), [2]Stony Brook University, Department of Geosciences, 255 Earth and Space Science Building, Stony Brook, New York, 11794-2100 (Deanne.Rogers@stonybrook.edu).

Introduction: An abundance of sedimentary units have been identified on Mars [1,2,3,4,5,6]. In terrestrial systems, sedimentary rocks are complex mixtures of multiple mineral phases, grain sizes, cements and textures, that are all related to the formation, diagenesis, weathering and erosion of the rock itself. Often, microcrystalline minerals are present within these rocks and are strongly indicative of specific diagenetic environments or processes. Common micro-crystalline components of sedimentary rocks are silica (chert), carbonate (micrite) or gypsum (alabaster), and their presence, or absence, can suggest certain depositional or diagenetic processes. For example, microcrystalline quartz is a common chemical precipitate (fumerolic or biogenic) or alteration product [7]. Conversely, macrocrystalline quartz is typically a primary phase. Microcrystalline carbonate can form in a variety of depositional environments, but is most abundant when precipitated in shallow and still, sub-tidal waters by organic or inorganic processes [8]. Microcrystalline gypsum typically forms as a secondary or fibrous phase after the original gypsum formed, was later uplifted or exhumed, and eventually came into contact with near-surface fluids [9].

Given the importance of the presence of these phases to the depositional and diagenetic history of sedimentary rocks, it is clear that the ability to distinguish between micro-crystalline and macro-crystalline phases using remote analyses would be a useful tool for understanding depositional and post-deopositional environments on Mars.

In thermal infrared spectra, differences between some cherts and macro-crystalline quartz have been noted in previous studies [10,11,12,13]. Others have noted the "pointed" restrahlen features associated with quartz in banded iron formation (BIFs) [14]. Bridges et al. 2008 suggested the features were related to "fine polycrystalline grain fabrics and associated thin iron oxide coatings" [15]. Michalski et al. attributed these features to roughness effects [13]. The motivation behind this study is to understand the underlying cause of these differences.

Here, we show that (a) microcrystalline minerals exhibit naturally rough surfaces compared to their macrocrystalline counterparts, at the micron-scale; and that (b) this roughness causes distinct spectral differences within the restrahlen bands of each mineral.

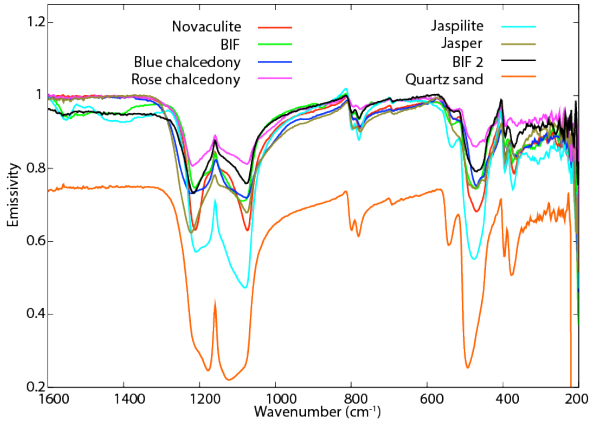

Figure 1. Emissivity spectra for a variety of microcrystalline quartz samples. Note that the shape of the spectral features within the restrahlen band (1050-1200 cm^{-1}) in the Jaspilite spectrum more closely resemble crystalline quartz (Quartz sand) than the other microcrystalline samples.

Methods and Results: We chose to work with a diverse set of microcrystalline samples. All samples were cut into thin sections for crystal size analysis. The resulting thin section stubs were polished with 1 µm grit on a polishing wheel. Natural surfaces of each sample were unmodified. Emissivity spectra and laser topography profiles were acquired for both natural and polished surfaces.

Thermal Infrared Spectral Data Acquisition: Analyses were conducted at the Vibrational Spectroscopy Laboratory (VSL) in the Department of Geosciences at Stony Brook University. The Thermo Fisher Nicolet 6700 FTIR spectrometer is modified to collect emissivity spectra in an environment purged of water vapor and CO_2. Emissivity spectra for many microcrystalline quartz samples are shown in **Figure 1,** and compared with macrocrystalline quartz particles.

Surface Topography Measurements: Surface topography was acquired from six samples using a Zygo laser profiler. To increase reflectivity from the samples, the samples were sputter-coated with a CoCrMoAu alloy. Surface topography was acquired over six separate ~85 x 64 µm areas on each sample, using a step size of ~0.26 µm. Areas of missing data are due to large differences in topography (e.g. "benches" or "stair-steps") on the sample surface, or, less commonly areas of very high roughness at visible wavelengths, which scatters the laser radiance and produces low return signal.

Multiple scales of roughness are present on any surface. In this work, because we are investigating roughness effects at the scale of the wavelength (~10 µm), we calculate roughness at the 10 µm scale. Raw elevations (z, in µm) were first smoothed using a 10 µm boxcar filter. Then, the smoothed data were subtracted from the raw elevation data (**Figure 2**). This provides a detrended roughness with a 10 µm baseline value (z_{10}), where a neutral height is equal to 0.0 µm. Data dropouts were not included in the running average by the boxcar filter. Next, R_a values on the 10-µm roughness data (excluding null/missing data values) were calculated on a line-by-line and column-by-column basis (referred to as "Ra_{10}" values in this work). The frequency distributions for all R_{a10} values in the row and column directions for all six images are displayed as box and whisker plots in **Figure 3**. This allows one to view the range of R_{a10} values rather than selecting R_{a10} from a line or column at random.

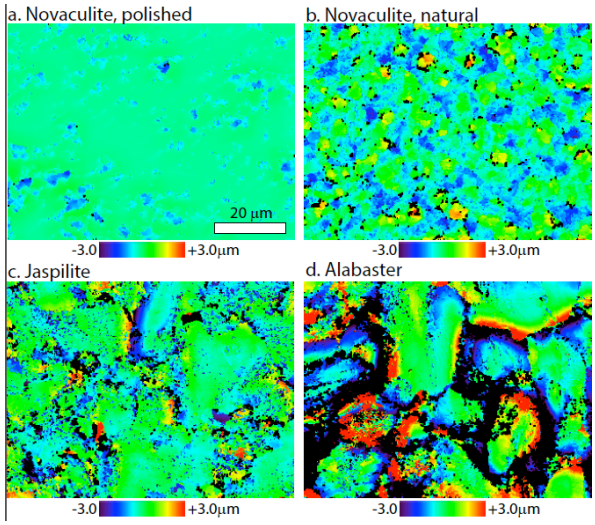

Figure 2. Detrended surface topography data. (a) novaculite polished, (b) novaculite natural, (c) jaspilite and (d) alabaster. Elevations are in µm. Note strong elevation gradients near crystal face boundaries in the alabaster sample; these are artifacts resulting from stair-steps that are not captured in the detrending process.

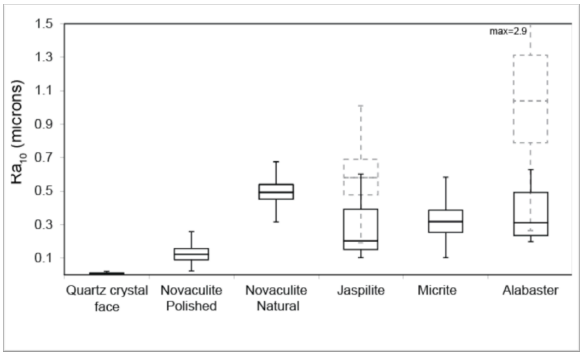

Figure 3. Frequency distributions of R_{a10} values for the six samples measured with a laser profiler. The top and bottom of each box represents the 25th and 75th percentile value, the horizontal line represents the median value, and the whiskers represent the min and max value. The box-and-whiskers from the quartz crystal face, novaculite polished and natural, and the micrite samples were generated from 3360 z_{10} profiles, representing all available data. The dashed box-and-whiskers from jaspilite and alabaster were also generated from 3360 z_{10} profiles. The solid box-and-whisker plots for jaspilite and alabaster were generated from 12 z_{10} profiles selected from individual crystal faces.

Discussion: We find that the changes in spectral shape occur for all samples at R_{a10} values >0.2 µm. This suggests that when observing natural surfaces using thermal infrared spectroscopy, assessments of the surface roughness of the sample can be made by analyzing changes in shapes of primary spectral features.

We find that samples with crystal sizes greater than ~25 µm do not display a change in spectral shape. For surfaces that were polished to a roughness of ~1 µm, the effect was also not observed, indicating that surface roughness (perhaps due to the size of the crystals themselves) of the sample itself dominates the shape of the spectral features for each phase. We do observe a spectral shape change for our micrite sample, which has a maximum crystal size of ~5 µm, suggesting that the spectral shape transition occurs between 5 – 25 µm crystal sizes. Note that no spectral changes are observed in wavelength regions where the absorption coefficient (k) is low. The observed spectral effects are thus attributed to multiple surface scattering. With each spectral reflection, a small portion of energy is transmitted into the grain. Thus with increasing surfaces of reflection, more incident energy will be lost [16].

References: [1] Bibring et al., Science, 307, 2005 [2] Gendrin et al., Science, 307, 2005 [3] Poulet et al., Nature, 438, 2005 [4] Michalski and Noe Dobrea, Geology, 35, 2007 [5] Milliken et al., LPSC Abs. 2025, 2008 [6] Grotzinger et al., Science, 343, 2013 [7] Knauth, Reviews in Mineralogy, 29, 1994 [8] Flugel, Microfacies of Carbonate Rocks, 2nd edition. [9] Tucker, Sedimentary Petrology, 3rd edition. [10] Michalski et al, 2003 [11] Ruff et al, 2011 [12] McDowell M., *dissertation*, U. Hawaii, 2009 [13] Michalski, *dissertation,* ASU, 2005. [14] Crowley et al. LPSC Abs. 1263, 2008. [15] Bridges et al, EOS 89, 36, 2008. [16] Thompson and Salisbury, Remote Sensing of Environment, 45, 1997.